15 September 2002

Optics Communications 210 (2002) 149–154

OPTICS COMMUNICATIONS

www.elsevier.com/locate/optcom

A photonic device compatible process in fabricating tunable Fabry–Perot filter

W.T. Lin[a], J.C. Chiou[a,*], Bruce C.S. Chou[b]

[a] *Department of Electrical and Control Engineering National Chiao Tung University, HsinChu 300, Taiwan*
[b] *Precision Instrument Development Center (PIDC), National Science Council, Taiwan*

Received 11 January 2002; received in revised form 30 April 2002; accepted 18 June 2002

Abstract

A photonic device compatible low temperature process that is suitable for fabricating tunable Fabry–Perot filter is proposed in this paper [1]. The advantages of the presented process consist of (1) materials used in this process are compatible with existing optical or IC process; (2) process and detected spectra are not limited by different substrates. Experimental results of the manufactured tunable Fabry–Perot filter indicated that the full-width-half-maximum (FWHM) is closed to 1.3 nm and the measurement of reflectance of distributed Bragg reflectors is up to 99%. Note that within the 10 nm experimental tuning range, the FWHM is kept close to 1.3 nm with tuning voltage from 0 to 30 V. The experimental results showed that the presented process has potential to apply to wavelength division multiplexing (WDM) specifications of optical telecommunication. In particular, the process would also be integrated to fabricate tunable VCSEL processes. © 2002 Elsevier Science B.V. All rights reserved.

1. Introduction

For a wavelength division multiplexing (WDM) networking system, tunable optical filters, that play an important role as the increased number of wavelengths (channels) transmitted into a single fiber. It means that more and more information added and dropped at various and exchanged between optical core networks or region access networks. In realistic applications, tunable optical filters must satisfy requirements such as wide tuning range, constant gain, narrow bandwidth and fast tuning. Since tunable Fabry–Perot filters could match the above-mentioned requirements well, thus, they would have been widely used in WDM systems.

In general, there are different methods and concepts to fabricate tunable Fabry–Perot filters using micro-electro-mechanical systems (MEMS) technology. These methods consists of: (1) bulk micro-machined technology incorporating with wafer bonding technology [2,3]; (2) surface micro-machined technology with polyimide as the sacrificial layer [4,5] and (3) VSCEL process with GaAs epitaxy as the sacrificial layer [6–8]. These approaches run into drawbacks such as high driving voltage, poor parallelism between two distributed

---

[*] Corresponding author. Tel.: +886-3-5731881; fax: +886-3-5715998.

E-mail address: chiou@cc.nctu.edu.tw (J.C. Chiou).

PII: S0030-4018(02)01691-7

Bragg reflector mirror, complex fabricating processes and uncontrollable or limited of resonant cavity length. Furthermore, all of the above-mentioned methods are constrained by the substrates, high process temperature and complex fabrication process. In order to overcome the above-mentioned drawbacks, a low temperature surface micro-machined technology that is suitable for fabricating tunable Fabry–Perot filter is proposed. In particular, the present process is not limited by any substrates that can also be integrated to fabricate tunable VCSEL.

2. Designs and fabrication

The fundamental structure of Fabry–Perot filter comprise of a resonant cavity that is formed between two high reflectance distributed Bragg reflector (DBR) mirrors. The properties of Fabry–Perot filter are decided by the well-known Airy formula ($A(\theta)$), the resolving power ($\Re$) and free spectrum range (FSR) [9]

$$A(\vartheta) = \frac{I_t}{I_i} = \left(\frac{T}{1-R}\right)\frac{1}{1+[4R/(1-R)^2]\sin^2(\delta/2)}, \tag{1}$$

$$\Re = \frac{\lambda_0}{\Delta\lambda_0} \approx \frac{\pi\sqrt{R}}{(1-R)}\frac{2n_f d}{\lambda_0}, \tag{2}$$

$$\mathrm{FSR} \approx \lambda^2/2n_f d \propto \frac{1}{d}, \tag{3}$$

where δ is the phase arising, R is the reflectance of DBR, d is the optical resonator length, λ_0 is the center wavelength, and n_f is the refractive index.

For the DWDM applications, filters are used to obtain sharper transmission wavelength in order to separate more channels, which can be accomplished by increasing the optical resonator length and the reflectance of DBR. However, by increasing the optical resonator length that will decrease the FSR range and increase driving voltage and consequently affect the filters' tuning range. Therefore a suitable optical resonator length and high reflectance of distributed Bragg reflector mirror are the most important parameters in designing a high quality Fabry–Perot filter. In the present proposed process, the designed device consists of 1.6 μm optical resonator length and DBR has a reflectivity of about 99.5% from approximately 1.35 to 1.6 μm as measured in Fig. 1. Note that the calculated theoretical FSR is about 750 nm and FWHM is close to 1.2 nm.

The schematic Fabry–Perot filter structure is shown in Fig. 2. The proposed filter consists of an optical mirror on silicon substrate and a floating bridge structure with another optical mirror that is formed on top of floating bridge. The electrostatic force is used to adjust the optical resonator length with a driving voltage that is applied to the top and the bottom electrodes in order to tune needed resonant wavelength. According to the optical transmission characteristics, when the air gap

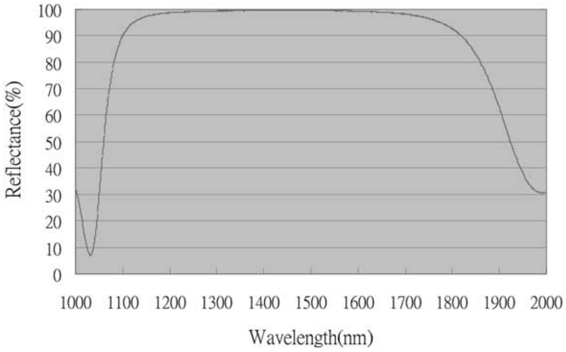

Fig. 1. The reflectance measurement result of the DBR.

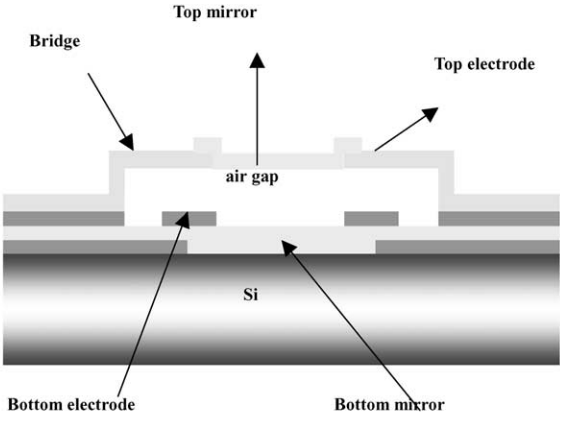

Fig. 2. The scheme of surface micro-machined filter.

equals multiplicity of a half-wavelength of the incident broadband light, which will enable to filter the suitable wavelength with a sharp resonant transmission peak passing through the two parallel mirrors. The optical resonator length of the device is designed for a center wavelength of 1550 nm. In order to realize the proposed optical filter, a new low temperature fabrication process is summarized in Figs. 3(a)–(f).

First, we deposited titanium to isolate the useless light and patterned an aperture to force light pass through it. Next, the bottom mirror was deposited on titanium isolator as shown in Fig. 3(a). In Figs. 3(b)–(c), we deposited and patterned titanium as the bottom electrodes, then deposited aluminum to be the sacrificial layer. Note that the critical issue of the present processes is the use of aluminum that is standard material used in IC process. Note that the material properties and parameters of deposition rate of aluminum have been completely understood which can be used to control its thickness accurately for optical resonator length. E-gun was used here to deposit the sacrificial layer and to ensure the design requirements could be matched accurately. With the lower mirror and the sacrificial layer, we further used E-gun to deposit seven overlapping layers of Ti/Au layers, which are 1000 and 8000 Å, respectively, as shown in Fig. 3(d). Note that the Ti/Au layers are compatible with any existing optical processes that can be are used to form the bridges and membrane. The purpose of using Ti/Au layers is to compensate its individual material stiffness properties. Furthermore, in order to eliminate the residual stress between the layers, we place the fabricated filter in the N_2 gas chamber at 200 °C for 30 min to complete its annealing process. As shown in Fig. 4, we observed the difference between the released bridges with or without the residual stress due to annealing. In the Fig. 3(e), we

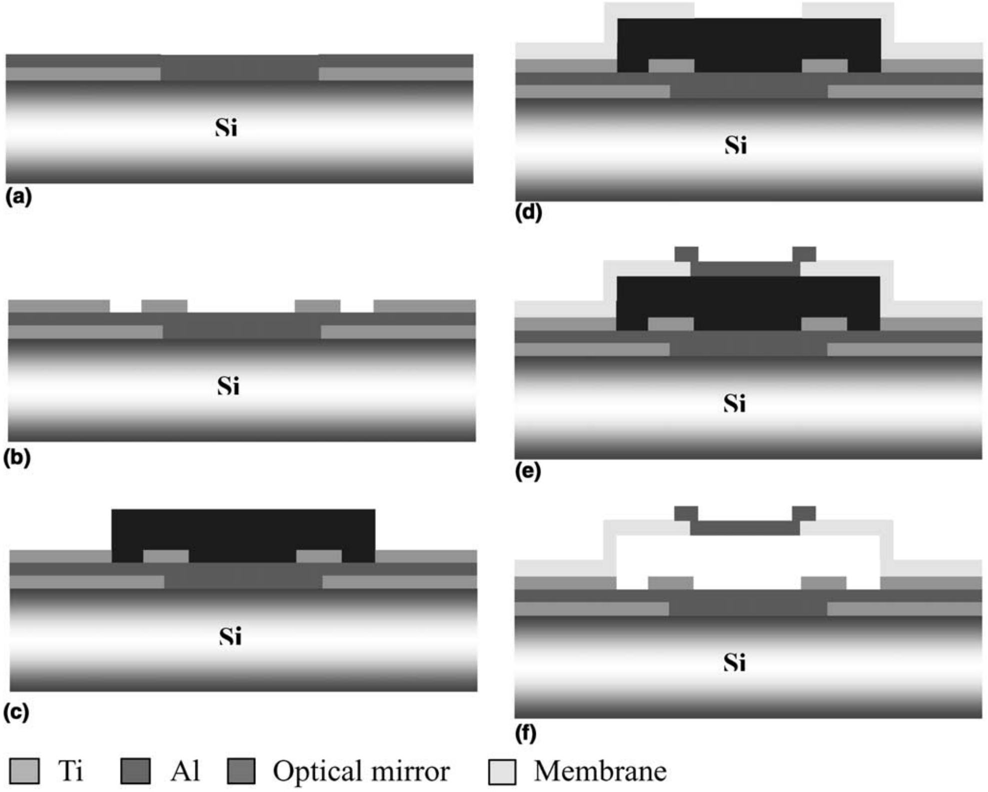

Fig. 3. (a)–(f) Summary of the fabrication process.

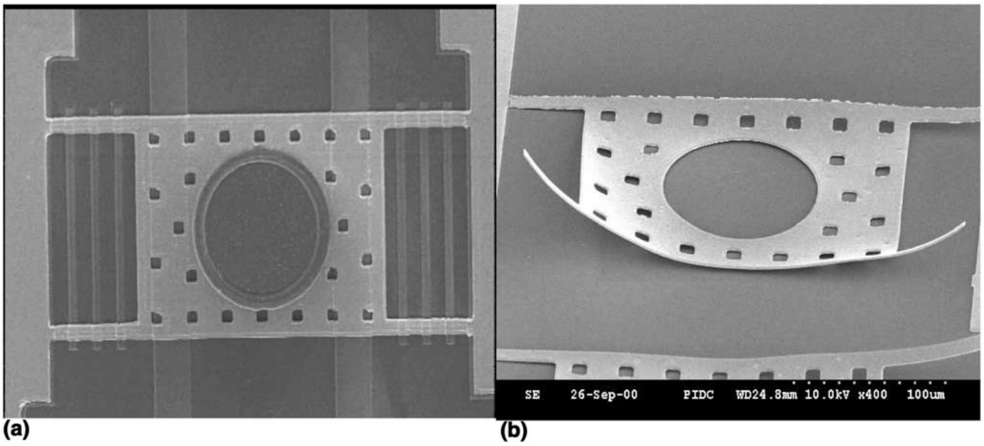

Fig. 4. SEM pictures of the membrane residual stress: (a) with annealing; (b) without annealing.

completed the deposition of the top mirror using left-off technology. To obtain the final Fabry–Perot filter, aluminum-etching solution is used to release the sacrificial layer as shown in Fig. 3(f). However the aluminum-etching solution also attacks titanium electrode resulting in the disappearance of top and bottom electrodes. Nevertheless, in order to avoid the etching of titanium, dissolving a grain of aluminum into the etching solution for a few minutes that would dramatically decrease the titanium-etching rate. Finally, we used methanol and hot plate to avoid the sticking phenomenon between membrane and substrate, which is shown in Fig. 5. It is note that the best method to avoid the sticking phenomenon is to use CO_2 critical point dryer. Note that all of the processes were fabricated by physical vapor deposition implying that if there have been existed photonic devices on substrate; the low temperature processes would not affect these devices.

Fig. 6 is the SEM picture of the Fabry–Perot filter with membrane area of 200 μm × 150 μm. The top and bottom mirror are circles in the center of the membrane with a diameter of 100 μm and on the substrate with a diameter of 120 μm, respectively. These mirrors compose of alternating $\lambda/4$ layers of Si and SiO_2 for the reason that they have large index contrast property and they are common materials used in semiconductor fabricating process. The structure of DBR composes of 3.5 pairs of Si and SiO_2 where the thickness is about 1076 and 2672 Å, respectively.

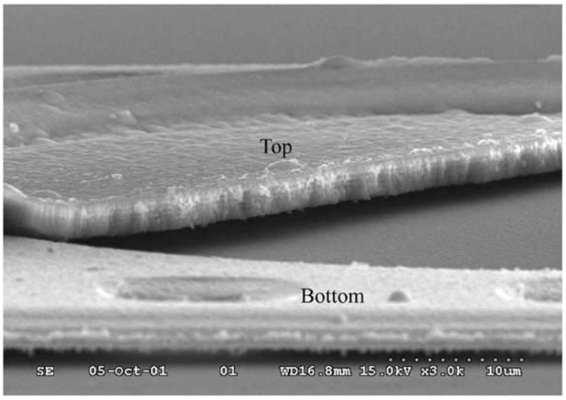

Fig. 5. The cavity of DBR (top) and membrane (bottom).

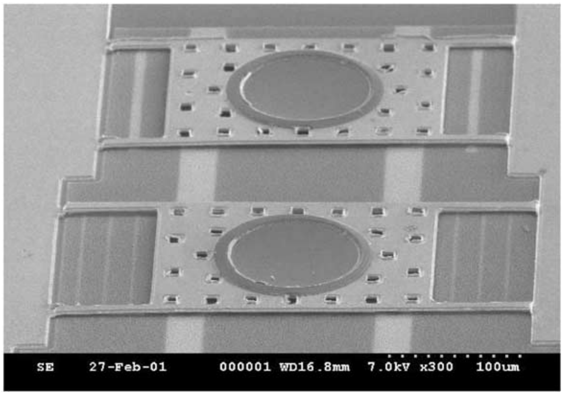

Fig. 6. The SEM picture of the Fabry–Perot filter.

3. Experimental results

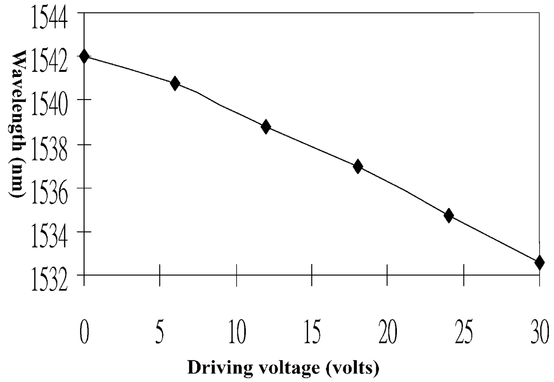

Fig. 7. The wavelengths versus bias voltages.

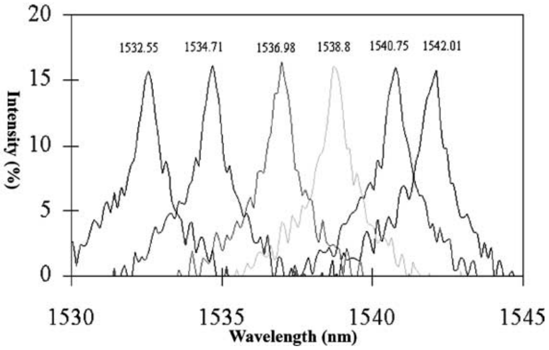

Fig. 8. The tuning wavelengths versus intensity.

In the present experimental setup, the ASE light was used as broadband light source in the 1550 nm region to verify the fabricated Fabry–Perot filter. The light beam was going through the fiber and collimator and lead into Fabry–Perot filter. The driving voltage was used to adjust the optical resonator length to filter individual transmission wavelength. The output light is collected by a lens transmitted through a multimode optical fiber and guided it to an optical spectrum analyzer ADVANTEST Q8347 for spectrum measurements. Fig. 7 shows the relationship between the wavelength output (1532–1542 nm) and the bias voltage (0–30 V) of the fabricated Fabry–Perot filter. The reason that we need a high bias electrostatic actuated voltage is due to the small electrode area. Fig. 8 demonstrates the relationship between light intensity and wavelength. Here in the 10 nm range, we are able to tune 5 output wavelength channels where the FWHM of the output wavelength peak is about 1.3 nm. This result matched the theoretical data closely.

However, the transmission wavelength intensity (15–20%) is not performed well as our anticipating. This is due to the reasons that: the membrane may tilt slightly during the stage of applying the driving voltage to the membrane and consequently loss the incident-light intensity. Furthermore, since the fabricated Fabry–Perot filter does not coat with anti-reflection layers on the backside of the wafer, which may produce a decayed light intensity through wafer. Fig. 9 indicated that the re-

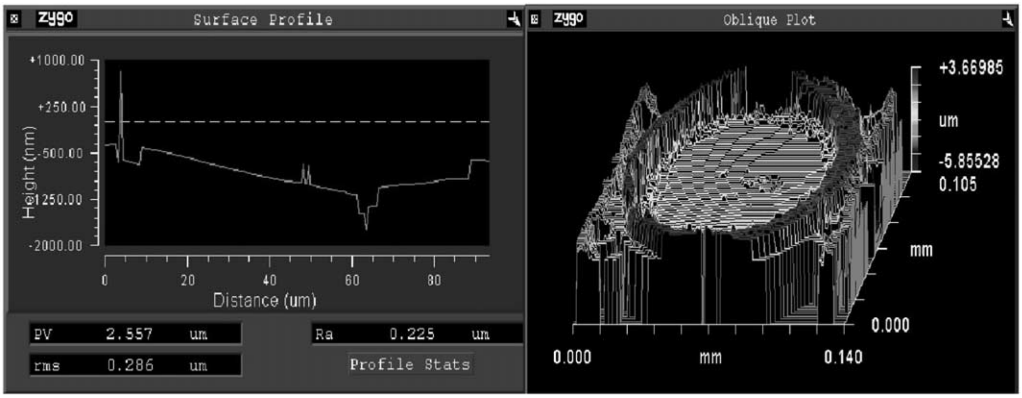

PV 2.557 um
rms 0.286 um
Ra 0.225 um

Fig. 9. The flatness of DBR measured by Zygo interferometer.

sidual stress of DBR mirror would produce 0.225 μm average flatness error. This error is larger than $\lambda/4$ of the light source from Zygo interferometer which affect the light intensity in our experiment with ASE light source. In conclusion, the overall performance of the filter is strongly affected by the above-mentioned behaviors. Although not report herein, a further investigation is under study in regard to eliminate these drawbacks. We will report this effort in the near future.

4. Summary

In this paper, a ultra-low temperature (<200 °C) fabrication process for micro-machined tunable filter has been proposed with proven feasibility. With the low temperature property, the process could be used to suit different substrates and their detected spectrum is not limited by any substrates although our device is fabricated on silicon substrate here. Note that the present process is compatible with any existing optical or IC process. The fabricated tunable Fabry–Perot filter based on a high reflectance DBR, which is up to 99%, low stress membrane, and suitable driving voltage that produced a small FWHM of 1.3 nm. This low temperature MEMS process has the potential to integrate with other existing photonic devices such as tunable VCSEL. Moreover, a high quality Fabry–Perot filter could be used as a key component of interferometer or spectrometer.

Acknowledgements

The authors would like to thank Dr. Hui-Hsiung Lin and Dr. Jer-Wei Chang of Precision Instrument Development Center (PIDC), National Science Council, ROC for the configuration of the optical testing and suggestions in filter designs and fabrications. The present work was supported by the National Science Council under Grant NSC 90-2215- E-009-101; and EX-91-E-FA06-4-4.

References

[1] W.T. Lin, Bruce C.S. Chou, J.C. Chiou, in: The Conference of 2001 IEEE/LEOS Optical MEMS, 2001, p. 71.
[2] N.F. Raley, D.R. Ciarlo, J.C. Koo, B. Beiriger, J. Trujillo, C. Yu, G. Loomis, R. Chow, Solid-State Sensor and Actuator Workshop, 5th Technical Digest, IEEE (1992) 170.
[3] J. Peerlings, A. Dehe, A. Vogt, M. Tilsch, C. Hebeler, F. Langenhan, P. Meissner, IEEE Photon. Technol. Lett. 9 (9) (1997) 1235.
[4] P. Tayebati, P. Wang, M. Azimi, L. Maflah, D. Vakhshoori, Electron. Lett. 34 (20) (1998) 1967.
[5] A.T.T.D. Tran, Y.H. Lo, Z.H. Zhu, D. Haronian, E. Mozdy, IEEE Photon. Technol. Lett. 8 (3) (1996) 393.
[6] E.C. Vail, M.S. Wu, G.S. Li, L. Eng, C.J. Chang-Hasnain, Electron. Lett. 31 (3) (1995) 228.
[7] A. Spisser, R. Ledantec, C. Seassal, J.L. Leclercq, T. Benyattou, D. Rondi, R. Blondeau, G. Guillot, P. Viktorovitch, IEEE Photon. Technol. Lett. 10 (9) (1998) 1259.
[8] M. Strassner, J. Daleiden, N. Chitica, D. Keiper, B. Stalnacke, S. Greek, K. Hjort, Sensors and Actuators 85 (2000) 249.
[9] Eugene Hecht, in: Optics, third ed., Addison Wesley, UK, p. 409.